GROUP 2: NEW OPPORTUNITIES PRESENTED BY ADVANCES IN TECHNIQUES

Acta Cryst. (1995). B**51**, 432–446

Synchrotron Radiation – New Opportunities for Chemical Crystallography

BY MARJORIE M. HARDING

Chemistry Department, Liverpool University, PO Box 147, Liverpool L69 3BX, England

(*Received* 15 *June* 1994; *accepted* 29 *November* 1994)

Abstract

After a very brief description of synchrotron radiation (SR) sources and properties, a range of applications of SR to problems in structural chemistry is described. Powder diffraction with monochromatic SR now allows structure determination for compounds of moderate complexity (*e.g.* unit cells 10–15 Å); this can be valuable when good-sized single crystals are not available. Energy-dispersive diffraction, with a polycrystalline sample and using the continuous range of wavelengths in the SR beam, *i.e.* the 'white' beam, is well suited to the study of materials over a wide range of temperature or pressure, or to time-resolved studies. Monochromatic single-crystal diffraction has been used for structure determination and other studies of very small crystals; it has also been used for a variety of experiments where very high accuracy of all the data is important, including deformation density studies and space-group resolution. An account is then given of the Laue method, where the diffraction pattern of a stationary single crystal in the white SR beam is recorded, with exposure times of 1 s or less. It has been shown that good intensity measurements can be made from SR Laue diffraction patterns. They may, therefore, be used for structure determination of small crystals, or of short-lived crystals, but their greatest potential is likely to be in time-resolved studies.

Introduction

The first dedicated sources of synchrotron radiation (SR) came into operation in the early 1980s. Since then, SR has been widely exploited in physics, chemistry and biological sciences, and a third generation of synchrotron sources is coming into action. SR offers many new possibilities in crystallography; development for macromolecular crystallography and physics-based crystallography has led the way. This account is written primarily for the small moiety crystallographer who has not yet used SR, and it aims to illustrate a variety of applications in chemistry, rather than to give a full review of all the experiments that have been done.

The simplest synchrotron ring consists entirely of bending magnets and straight sections (Figs. 1 and 2) and the curve labelled SRS(BM) in Fig. 3 represents the

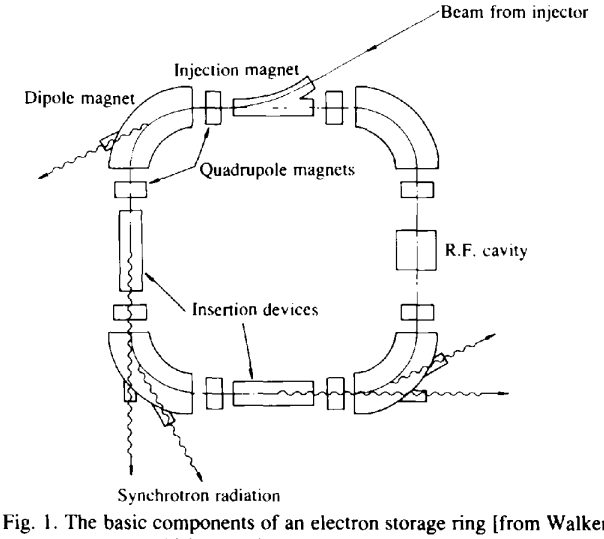

Fig. 1. The basic components of an electron storage ring [from Walker (1986); actually JRH's book, p. 103].

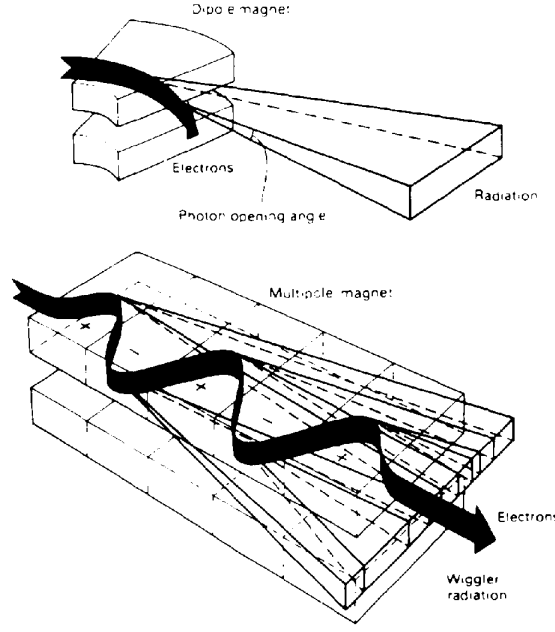

Fig. 2. Schematic representation of an electron beam and radiation emitted by dipole magnet (bending magnet) and wiggler magnets [from Catlow & Greaves (1990), p. 5].

distribution of X-ray intensity with respect to wavelength for one such ring. The distribution is shifted to shorter wavelengths by higher electron energy in the ring or by a smaller radius of curvature at the bending position, leading to the various distributions shown in Fig. 3. The synchrotron ring may also include insertion devices: with a wiggler, effectively three or five tight bends in alternate directions, greater intensity is available and its distribution is shifted to shorter wavelengths [Figs. 2(*b*) and 3]; with an undulator, much of the intensity may be concentrated in a small wavelength range (Fig. 4). Thus, two characteristics of the X-rays available are very high intensity and a continuous range of wavelengths. A third valuable characteristic is the very low beam divergence, especially in the vertical plane, compared with radiation derived from a normal X-ray tube as source. Fourthly, the radiation is plane-polarized, although this is a property of which comparatively little use has been made up until now; fifthly, the energy is delivered in pulses and some experiments will make use of this time structure.

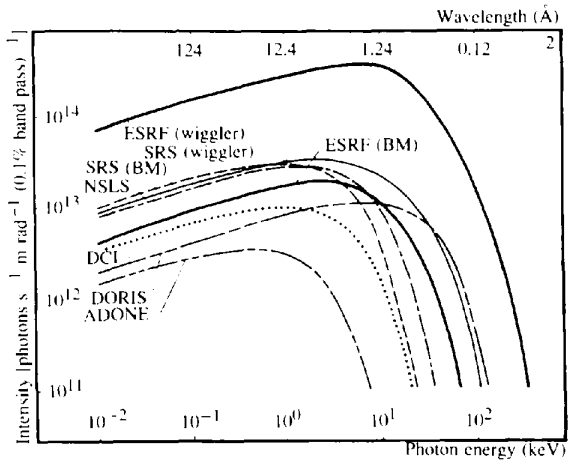

Fig. 3. Spectral intensity distributions for bending magnets and wigglers at various synchrotron radiation sources (ESRF = European Synchrotron Radiation Facility; SRS = Synchrotron Radiation Source, Daresbury, England; NSLS = National Synchrotron Light Source, Brookhaven, USA; DCI, Lure, France; ADONE, Frascati, Italy) [from Catlow & Greaves (1990), p. 7].

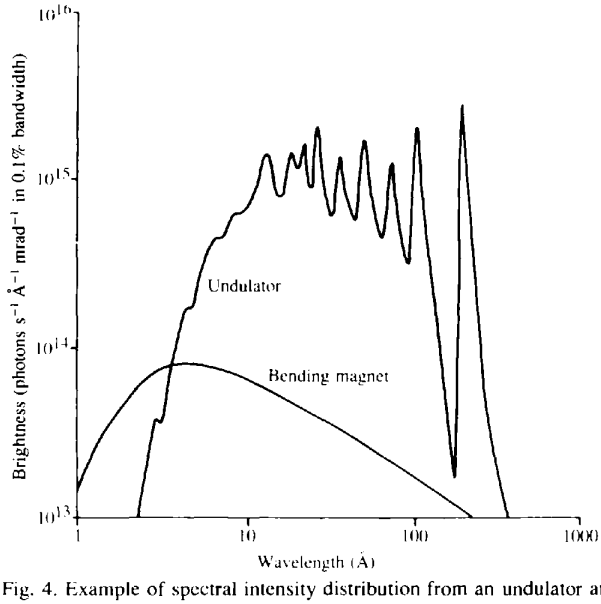

Fig. 4. Example of spectral intensity distribution from an undulator at SRS compared with that for a bending magnet. Undulators can be designed to concentrate most of the energy into quite a small wavelength range [from Catlow & Greaves (1990), p. 12].

Instrumentation

The chemical crystallographer would probably like simply to put his diffractometer up against this intense source and get on with measurements, but it is not as simple as that! At every synchrotron source there is a large group of people involved in the development, installation and maintenance of all the necessary instrumentation. For the source itself this includes vacuum technology, magnets and their cooling systems, electron beam injection, steering and control, monitoring of electron beam *etc.* For each beamline it also includes optics, *i.e.* monochromators and focussing mirrors (see Fig. 5, for example), safety systems with extensive interlocks, remote control for all alignment and other operations, detectors. I am not qualified to describe these in detail, but it is important to recognize how essential they are to all users. Fuller descriptions can be found in Helliwell (1992), Catlow & Greaves (1990), Coppens (1992), and Sweet & Woodhead (1989), as well as literature from the various synchrotron facilities and *J. Synchrotron Rad.* (Hasnain, Helliwell & Kamitsubo, 1994).

Much effort in the last 15 years has been given to developing facilities for single-crystal macromolecular crystallography (notably by J. R. Helliwell and by K. Moffat) and for powder diffraction (D. Cox and R. Cernik, for example), but it seems to me that only more recently has development effort been given to single-crystal experiments with small molecules. Moreover, there will always be a time lag between the introduction of a new facility, such as an undulator, and its routine use in a range of experiments to give chemical information.

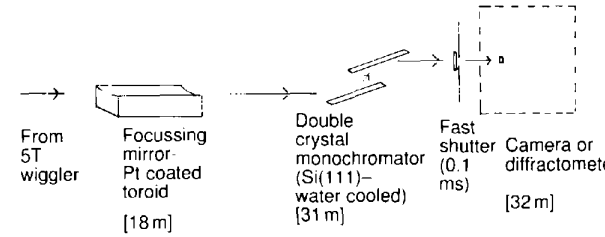

Fig. 5. A schematic example of beamline layout, SRS protein crystallography station 9.5.

Different types of experiments

The first broad division is between powder and single-crystal diffraction experiments, and within each group, between those which use monochromatic radiation and those which use the continuous range of wavelengths available, often described as the full 'white' beam. The monochromatic experiments are the analogues of conventional powder and single-crystal experiments, while energy-dispersive diffraction (EDD) for powders and the Laue method for single crystals use the full white beam. The obvious advantage of the white beam is the high intensity available, not diminished by monochromators *etc.*, but the fact that the sample and detector are stationary can be advantageous for experiments in special environments such as pressure cells, furnaces *etc.* Here I intend to survey powder diffraction work rather briefly, for there are good recent reviews (Cheetham & Wilkinson, 1992; Cox, 1992), and give more time to single crystal work. Of course, synchrotron radiation is contributing to structural chemical knowledge in other areas too, particularly EXAFS and surface diffraction.

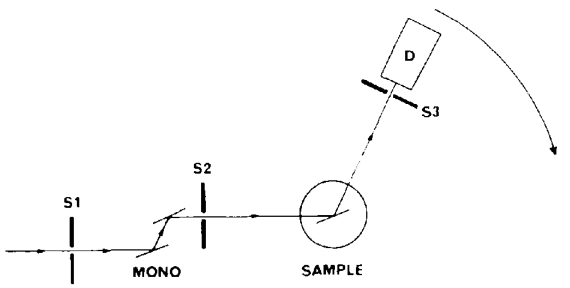

Fig. 6. Schematic illustration of high-resolution powder diffractometer at a SR source. S1, S2 and S3 are slits, D the detector may be at *ca* 1 m from the sample [from Catlow & Greaves (1990), p. 45, Fig. 2.2].

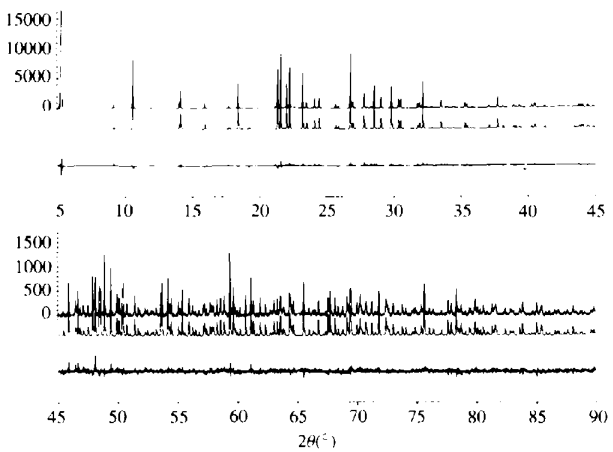

Fig. 7. Observed (upper), calculated (middle) and difference (bottom) powder diffraction profiles for the aluminophosphate VPI-5. (To show more detail, the first peak of the pattern has been cut at approximately 1/4 of its maximum intensity, and the second half of the profile scaled up by a factor of eight.) The first part of the pattern, to $2\theta \simeq 30°$, gives well resolved peaks appropriate for indexing and structure solution; the whole pattern, to $2\theta = 90°$, can be used for Rietveld refinement [from McCusker (1991), p. 308, Fig. 11].

Table 1. *Structure determination of the clathrasil sigma-2, from SR powder diffraction data (McCusker, 1988)*

Unit cell contents : 4 $Si_{16}O_{32}.C_{10}H_{17}N$
NSLS, Brookhaven, wavelength 1.54 Å
2θ 8.5–73° in steps of 0.01°
Peaks 0.04–0.08° (FWHM)
Space group $I4_1/amd$
Unit cell $a = 10.238$, $c = 34.382$ Å
258 independent reflection intensities extracted (but 26 of these severely overlapped)
Direct methods → 4Si and 5/7 framework O
Remaining Os and aminoadamantane (disordered) by difference map
Rietveld refinement 451 contributing reflections, 47 structural parameters, e.s.d.s of framework atoms to *ca* 0.01 Å (the structure is a zeolite-like framework, but with cages and not channels)

Monochromatic powder diffraction

The high intensity and low beam divergence of synchrotron radiation have allowed the design of powder diffractometers which give greatly enhanced resolution compared with conventional experimental arrangements (see Fig. 6, for example). The resulting diffraction pattern (*e.g.* Fig. 7) can be analysed to give θ angles accurate to 0.01° and integrated reflection intensities for each line. As a result, the indexing of a powder diffraction pattern and the derivation of the unit cell have become practical for larger cells and cells of lower symmetry than hitherto. This is followed by intensity measurement for as many lines as can be resolved and indexed – and programs such as Pawley's *ALLHKL* assist greatly at this stage (Pawley, 1981). In favourable cases the space group and then a structural model can be derived, for example by direct methods or from a Patterson series. Once a structural model has been found, refinement by the Rietveld method can use the whole diffraction pattern to improve this model, so that those regions where the peaks overlap are used as well as the fully resolved peaks. The procedures were tested on known structures first, but have now allowed structure determination for a number of important compounds which could not be obtained as suitable single crystals; zeolites and aluminophosphates are notable examples, and it is very appropriate to illustrate this with the *ab initio* structure determination of 'sigma-2' by McCusker (1988).

The clathrasil, sigma-2, is a framework zeolite with cages rather than channels. Some details of the compound and the data are given in Table 1. Direct methods using the 258 reflection intensities extracted from the powder-diffraction pattern led to all four Si atoms and five of the seven framework O atoms in the asymmetric unit; subsequently, difference Fourier maps yielded the remaining O atoms and the atoms of the aminoadamantane molecule in the cage (which is disordered). Finally, Rietveld refinement of 47 structural parameters, using the whole observed pattern, to which

451 reflections contribute, was carried out. The final e.s.d.'s of the framework atoms were *ca* 0.01 Å. Since then other structures representing a wide range of structure types, organics, superconductors, various oxides, zeolites and aluminophosphates have been determined and/or refined in a similar way, for example, norbornane at 50 K (Fitch & Jobic, 1993), the aluminophosphate VPI-5 (McCusker, Baerlocher, Jahn & Bulow, 1991), and others listed by Cheetham & Wilkinson (1992). The structural behaviour of many semiconductors and other compounds under high pressure has been explored by Nelmes and colleagues (Nelmes & McMahon, 1994).

The extraction from the powder diffraction pattern of sufficient resolved reflections for the structure solution by direct methods or Patterson is probably the most crucial step; maximum entropy methods and other peak deconvolution procedures to improve the prospects at this stage are being developed (Estermann & Gramlich, 1993). The combination of different techniques can sometimes be helpful. In cases where the establishment of unit cell or space group from powder diffraction data alone is difficult because of the overlap of important reflections, electron diffraction or SR Laue diffraction may be helpful; with zeolites, ^{29}Si MAS NMR has given useful information (McCusker, 1991). Thus, SR has greatly extended the possibilities of structure determination from powder diffraction data to compounds with larger unit cells and more complex structures.

Energy-dispersive diffraction

Here we have a stationary powder sample, and a detector at a fixed angle, which is able to resolve the different energies (wavelengths) present (Fig. 8). This arrangement is particularly useful when temperature or pressure are to be varied or for time-resolved studies.

Energy-dispersive diffraction was used at the SRS, Daresbury (station 9.7), to observe changes in the structure of solid C_{70} at pressures between atmospheric and 25 GPa. A single f.c.c. phase is present at atmospheric pressure. At 0.35 GPa another phase appears and by 1 GPa the face-centred cubic (f.c.c.) phase is no longer present (Christides, Thomas, Dennis & Prassides, 1993). Another example (see Fig. 9) shows the powder-diffraction pattern as a metallic phase which crystallizes from its melt at 798 K. Patterns could be recorded at intervals of 10 s, and the energy range used was 15–45 keV (0.83–0.28 Å).

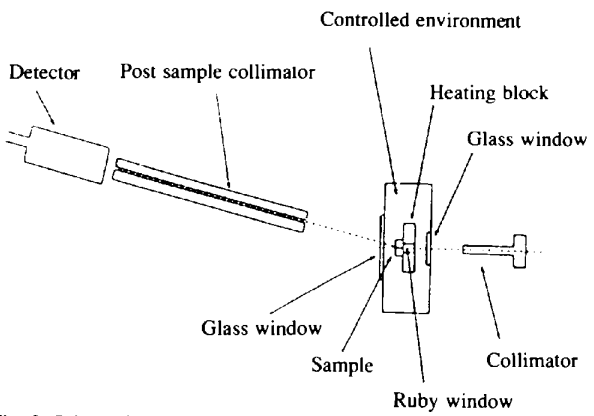

Fig. 8. Schematic diagram of energy dispersive diffraction experiment. The detector remains in a fixed position throughout the experiment [from Clark & Doorhyee (1992), Fig. 1].

Monochromatic single-crystal diffraction

The high intensity of SR makes its use for very small crystals an obvious application, and these have been studied for several purposes. Table 2(*a*) gives some examples. Schulz and coworkers in their pioneering study of very small CaF_2 crystals were concerned with establishing atomic displacement parameters of Ca and F in crystals where extinction effects were reduced or eliminated. Initially they used a four-circle diffractometer at Hamburg, and after mounting these very tiny crystals (with adhesive, on glass fibre) one of the difficulties was to locate the very small sharp diffraction spots – small because of the crystal size and the low beam divergence. In subsequent experiments at Cornell they used a multiwire area detector for this stage.

For the other crystals in Table 2(*a*), the aim has been structure determination, the establishment of chemical connectivity and/or constitution and stereochemistry; unit cells and structure were unknown before the experiments were carried out. The crystals are larger than the first group, but the unit cells are larger and more

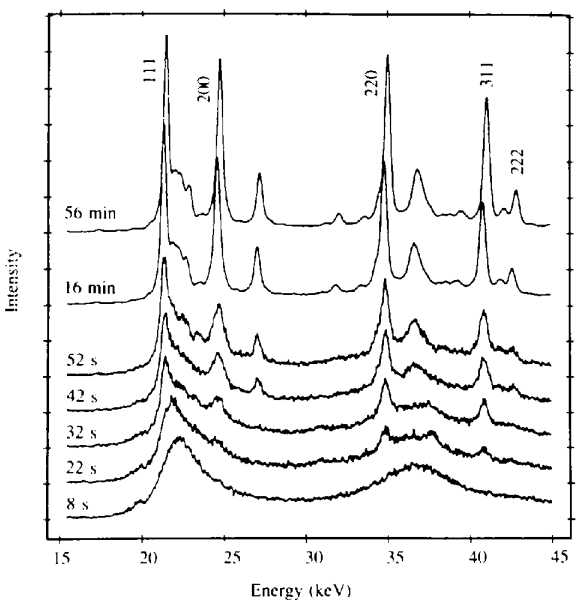

Fig. 9. A sequence of energy-dispersive diffraction patterns used to follow the crystallization of a metallic Fe,Ni phase from its melt at 798 K. 10 s was sufficient time to record profiles such as the lower ones shown [from Hausermann & Barnes (1992), Fig. 8].

Table 2. *Examples of the use of SR in single-crystal studies*

	Size (μm^3)	Objective	Wavelength (Å) location	Reference
(*a*) Small crystals				
Fluorite, CaF_2	6^3	Extinction free data, *B* values	0.91 Doris, Hamburg	(*a*)
Fluorite, CaF_2	2.2^3	Feasibility study	1.56 Chess, Cornell	(*b*)
Aluminophosphate, $AlPO_4$-CHA $Al_3P_3O_{12}F^-.C_4H_{10}NO^+$	35 × 20 × 15	Structure determination	0.9 SRS Daresbury	(*c*)
Organometallic gold cluster $Au_{10}(PPh_3)_7(S_2C_2(CN)_2)_2$	35 × 10 × 10	Structure determination	0.9 SRS Daresbury	(*d*)
Lipid model compound $NH_4^+.C_{18}H_{32}NO_6^-$	280 × 80 × 16	Structure determination	0.46 Doris, Hamburg	(*e*)
(*b*) Other crystals				
$Cr(NH_3)_6(CN)_6$	Deformation-density study (first with SR)		0.30 Chess, Cornell	(*f*)
K_2PdCl_4	Deformation-density study (one of a series)		0.70, 0.90 Photon Factory, Japan	(*g*)
Rubredoxin, small protein 400 non-H atoms + FeS_4	1 Å resolution data for structure refinement (previous best 1.5 Å)		0.65 Doris, Hamburg	(*h*)
Dodecasil-1*H* $(SiO_2)_n$	Accurate data to resolve details of disordered sites		0.79 Doris, Hamburg	(*i*)
Margarite $CaAl_2[Al_2Si_2O_{10}](OH)_2$	Good measurements of weak reflections to resolve space-group ambiguity		0.50, 0.60 Doris, Hamburg	(*j*)

(*a*) Bachmann, Kohler, Schulz & Weber (1985); (*b*) Rieck, Euler, Schulz & Schildkamp (1988); (*c*) Harding & Kariuki (1994); (*d*) Cheetham, Harding, Haggitt, Mingos & Powell (1993); (*e*) Lehmann *et al.* (1990); (*f*) Nielsen, Lee & Coppens (1986); (*g*) Hester, Maslen, Spadaccini, Ishizawa & Satow (1993); (*h*) Dauter, Sieker & Wilson (1992); (*i*) Miehe, Vogt, Fuess & Muller (1993); (*j*) Kassner *et al.* (1993).

complex. For comparisons we can estimate the average intensity of a reflection from

$$\langle F(hkl)^2\rangle.V_{\text{sample}}/V_{\text{cell}}{}^2,$$

and ignoring differences in atomic displacement parameters, $\langle F(hkl)^2\rangle = \Sigma f^2$. It turns out that the average intensity for the gold cluster crystal is comparable to that for the much smaller CaF_2 crystal, and also to that of the normal sized rubredoxin crystal!

For the gold cluster crystal and the aluminophosphate, the Enraf–Nonius FAST area detector diffractometer at Daresbury Laboratory (station 9.6) was used. Because discrimination of diffraction spot from background is difficult and important, we have mounted crystals in such a way that scattering by the normal stout glass mounting fibre does not occur (Fig. 10). Generally, it is essential to survey a number of crystals at the synchrotron and choose the best, because they are too small for quality to be judged optically under the microscope. The wavelength was *ca* 0.9 Å, and the whole diffraction pattern was recorded (or as much as time allowed) in frames of width 0.5–1°. The diffraction pattern could be seen on the monitor as it was recorded, but the processing of the images to give *hkl* and *F* values was carried out off-line. The processing used *MADNES* software (Messerschmidt & Pflugrath, 1987), with local adaptations to allow for the decay in incident beam intensity (continuously monitored and recorded), and polarization of the SR beam (Papiz, 1989). *MADNES* searches the whole diffraction pattern for spots, identifies and refines a unit cell and orientation, and then proceeds to integrate all the reflection intensities at the predicted positions. There was thus no difficulty in finding diffraction spots for these crystals, and in any case, for many of them the spots were quite streaked or enlarged, because the crystal mosaic spread was substantial; this is a characteristic we have found common in crystals of compounds which have failed to yield larger crystals suitable for a conventional diffractometer. The workstation had been developed for protein crystallography and the wavelength and many other aspects of the experimental arrangement were chosen to be optimal for that work, and they served our purposes fairly adequately.

The first compound listed [Table 2(*a*)] was known to be a gold cluster with triphenylphosphine ligands, an unexpected product of a reaction carried out by Professor D. M. P. Mingos and Dr Jane Haggitt. The crystals were too small for analysis by conventional diffractometer and only a small number were available. After some difficulty in identifying the unit cell, the Au atom positions were found by direct methods, and the Ph_3P ligands, and eventually the dithiolene ligands were identified from the geometry of the peaks in the difference map and a knowledge of the chemical preparation. By current standards it is not a particularly

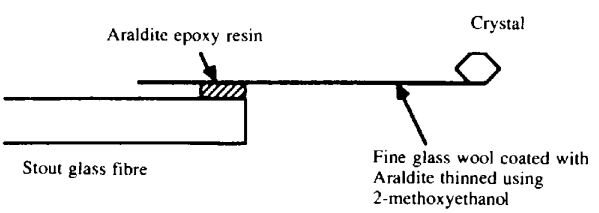

Fig. 10. Mounting of a very small crystal [from Rule (1990)].

accurate determination, and it would certainly have been better if a larger proportion of the theoretically available reflections could have been measured, but it has served its purpose and established the quite large and unexpected structure shown in Fig. 11.

The data for $AlPO_4$-CHA were similarly recorded, but are quite limited. The framework structure was fairly easily established, Al and P atoms could be distinguished by their electron densities; the F atoms were known to be present from chemical analysis and were assumed to be the atoms bridging pairs of Al atoms – a situation where O is not normally found. For this material Simmen and McCusker (Simmen, 1992) determined the structure from SR powder diffraction data; the bond length e.s.d.s from the two studies are comparable, but the single crystal data showed the atom positions of the template molecule slightly more clearly (Fig. 12).

We have been able to perform structure determinations of several other small crystals where conventional equipment has failed to obtain adequate data, for example, another organometallic complex (Harding, Kariuki, Mathews, Smith & Braunstein, 1994), the mineral aurichalcite (Harding, Kariuki, Cernik & Cressey, 1994) and chenodeoxycholic acid (Rizkallah, Harding, Lindley, Aigner & Bauer, 1990). The structure of the lipid bilayer compound listed in Table 2(*a*) was determined from data recorded at Hamburg with SR and a five-circle diffractometer; good quality diffraction data have clearly been obtained (refinement gave $R = 0.048$), but finding of the unit cell and orientation matrix was rather slow [Lehmann *et al.*, 1990; $R = \sum |(|F_o| - |F_c|)| / \sum |F_o|$ here and subsequently.

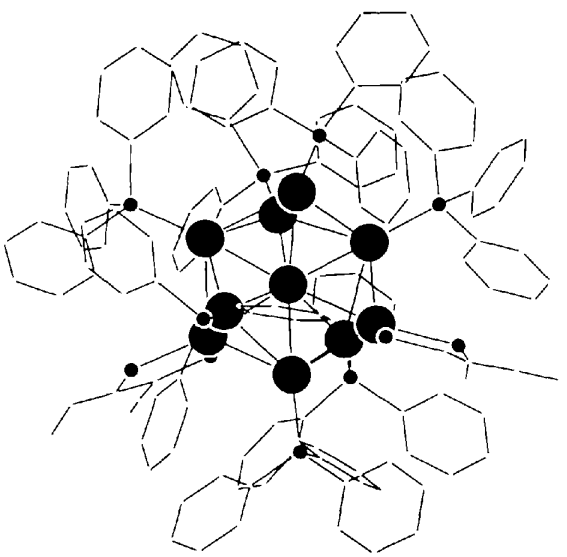

Fig. 11. A gold cluster compound, shown to be $Au_{10}(PPh_3)_7(S_2C_2(CN)_2)_2$. The compound crystallizes in space group $C2/c$, with eight molecules per cell. 15 391 reflection intensities were measured, merged to give 6470 unique, of which 3747 had $F > 6\sigma(F)$; for this structure, refinement gave $R = 0.064$. Large black circles are gold atoms, small circles are S or P.

For these small crystals the measuring of reflection intensities has always involved a struggle to measure signal against background, particularly when the mosaic spread is large and the peak width large despite the small beam divergence. Usually the smallest collimator available is *ca* 0.2 mm diameter, although this is ten times the diameter of some of the crystals; obviously a much smaller collimator should improve the signal-to-noise ratio, *provided* the mechanical accuracy of alignment of the collimator, crystal and diffractometer movements is good enough, but this is not easy to achieve. Microdiffraction systems are being developed which should greatly improve the prospects here (Bilderback, Thiel, Pahl & Brister, 1994).

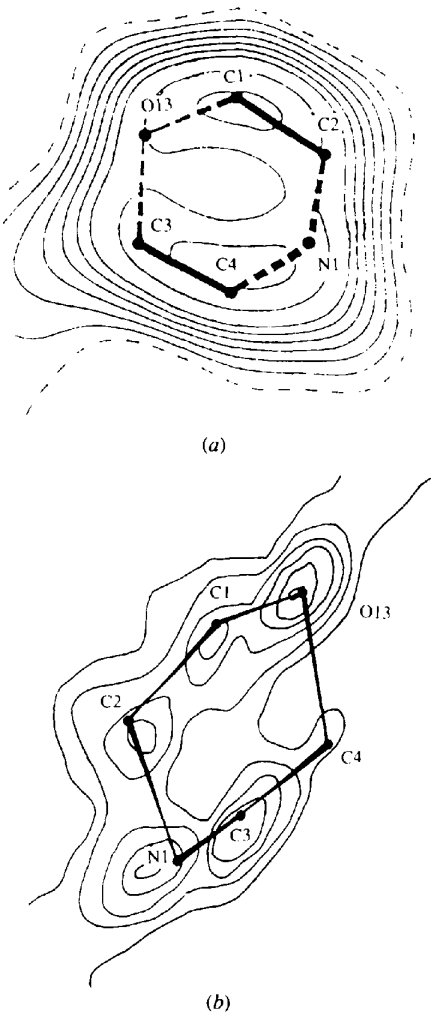

Fig. 12. Difference electron-density maps calculated for the location of the template morpholine ion, $C_4H_{10}NO^+$, in $AlPO_4$-CHA. (*a*) Calculated from SR powder diffraction data and (*b*) calculated from SR diffraction data from a very small single crystal (see Table 2). The compound crystallizes in space group $P\bar{1}$ with all cell edges *ca* 9 Å. In the single crystal study, 611 reflection intensities were measured, giving 590 unique, of which 289 had $I > 2\sigma(I)$; for these structure refinement gave $R = 0.081$ [(*a*) from Simmen & McClusker (1992)].

Table 2(*b*) gives examples of other uses of single crystal SR data. Rubredoxin is included as a representative of the very large number of macromolecular crystals that have been studied, and in this area SR data has already made an enormous contribution to structural knowledge. The high intensity and low beam divergence have led directly to more, and more accurate, intensity data, and consequently much clearer and more interpretable electron-density maps. The reduction in radiation damage by the use of shorter wavelengths, and because the data collection times are shorter, has also contributed much to the improvement in data quality.

The other examples in Table 2(*b*) show where this improvement in data quality and quantity has been used for chemical or 'small molecule' problems. In Coppens' pioneering study of the chromium complex, the very short wavelength 0.30 Å was chosen to minimize extinction and absorption, but there is a penalty – the diffracted intensities are much weaker because the scattering power of an atom falls off with λ^3, and because the source intensity is lower. Clear maps of the deformation density around all atoms were obtained. Similarly in more recent studies, Maslen has mapped deformation density in a variety of other compounds. In Fig. 13 deformation densities calculated from Mo $K\alpha$ data and SR data are compared, in the latter the features and background appear very much cleaner.

In dodecasil-1*H*, a complicated pattern of disordered oxygen sites has been resolved (Fig. 14). The mean Si—O—Si angle is 155°, and the SiO_4 tetrahedra can take several different but similar orientations. With more limited X-ray data from a conventional source, the Si—O—Si bonds appeared to be more nearly linear and larger anisotropic atomic displacement parameters were attributed to the oxygens. In margarite good measurements of the weak reflections, refinement using all reflections [not just those with $F > 3\sigma(F)$], and examination of the agreement of the weak reflections clearly showed that the space group was *Cc*, not *C*2/*c*.

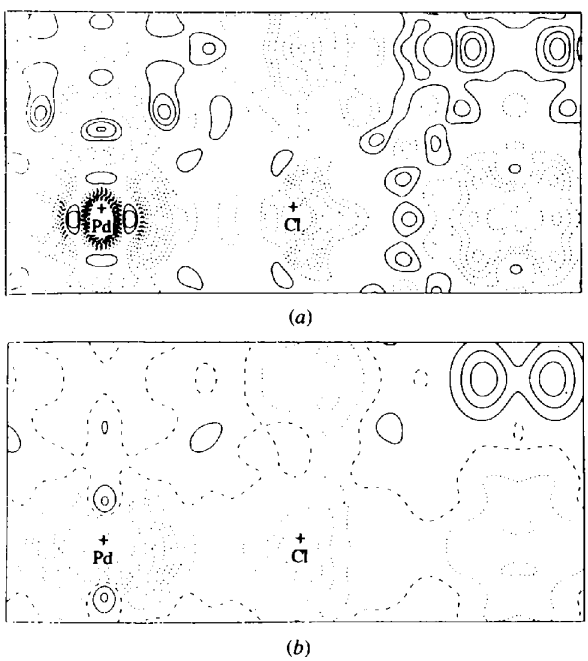

Fig. 13. Difference electron-density maps for the (110) plane of K_2PdCl_4. (*a*) is calculated from Mo $K\alpha$ data and (*b*) is calculated from SR data recorded at Photon Factory, Japan, using the wavelength 0.7 Å [from Hester, Maslen, Spadaccini, Ishiziwa & Satow (1993), Fig. 1].

Anomalous dispersion, monochromatic measurements

With SR, the wavelength and the bandpass ($\Delta\lambda/\lambda$) can be selected using a monochromator; the present practical wavelength range lies between *ca* 0.5 and 2.0 Å. Almost all elements heavier than Mn have an absorption edge within this range. Fig. 15 shows how in the vicinity

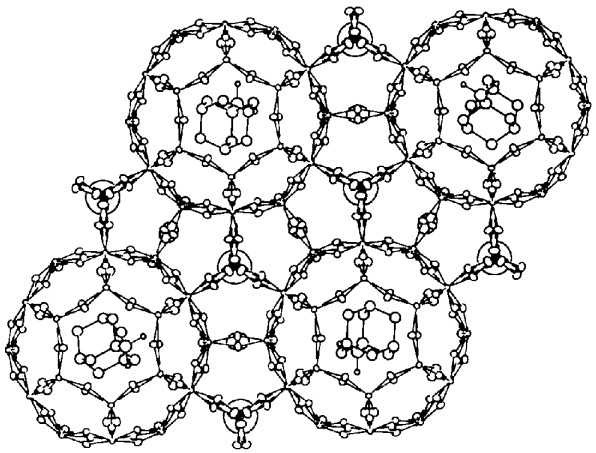

Fig. 14. Model of the structure of the SiO_2 host lattice of dodecasil-1*H* showing pairs of disordered positions for many of the O atoms. SR data allowed refinement of these split oxygen positions (giving $R = 0.026$ for 784 unique reflections), whereas Mo $K\alpha$ data had merely suggested large anisotropic vibration parameters. Guest molecules in the structure are also shown [from Miehe, Vogt, Fuess & Muller (1993)].

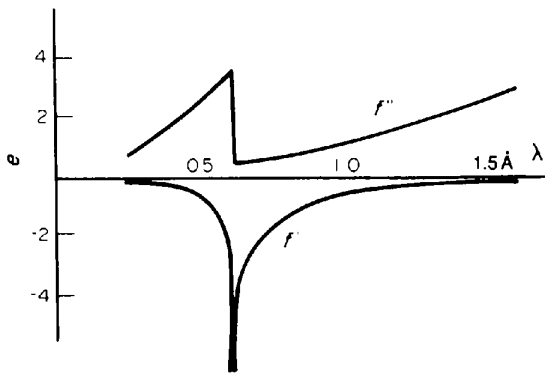

Fig. 15. The anomalous dispersion terms f' and f'' for Mo, calculated by the program *FPRIME* (Cromer & Liberman, 1970). For comparison f_{Mo} is 42 electrons at $\sin\theta/\lambda = 0\,\text{Å}^{-1}$, but only 22 electrons at $\sin\theta/\lambda = 0.50\,\text{Å}^{-1}$.

of an absorption edge the magnitudes of the two anomalous dispersion terms f' and f'', which modify the normal scattering factor f, can be substantial, for example up to 6 and 3.8 electrons for Br, 16 and 10 electrons for Pt. In protein crystallograhy multiwavelength anomalous dispersion (MAD) has been successfully used in a few cases for structure solution. Reflection intensities are measured at at least three, and more often four to six, carefully selected wavelengths for a protein crystal containing an anomalous scatterer, and the information is used to derive phases. Obtaining accurate enough measurements of the differences for successful structure solution is difficult, but no isomorphous derivatives or related structures are required. Hendrickson *et al.* (1989) have solved the structure of streptavidin, a 252 amino-acid protein including two Se atoms, by the MAD method, thus demonstrating that the method could be widely applied if seleno derivatives were (bio)synthesized in place of normal protein.

For simpler crystals there has been little need for this approach since other methods of phasing have become so effective. The Templetons did considerable pioneering work at Stanford, obtaining experimental values of f' and f'' in simple crystals and showing that they vary (slightly) with the state of chemical combination of the element concerned, and even with the orientation of the bonding pattern around it (see, for example, Templeton & Templeton, 1988; Templeton, Templeton, Phillips & Hodgson, 1980).

Using powder diffraction Wilkinson, Cheetham & Cox (1991) have shown that the difference in f' and f'' values (as well as the position of the absorption edge) for different oxidation states of an element can be detected. Powder data for $GaCl_2$, which is really $Ga^{I}Ga^{III}Cl_4$, were recorded at 1.1957 and 1.2478 Å, and five wavelengths between; at each wavelength values for f' and f'' were refined as well as the structural parameters, and then compared. Anomalous dispersion has also been used to distinguish elements of close atomic number using powder diffraction data, for example Bi and Sr when they occupy the same site in a superconductor (Petricek, Gao, Lee & Coppens, 1990).

The SR Laue method

In these experiments the crystal is stationary in the white beam. The experimental arrangement appears simple (Fig. 16) and it is comparatively easy to incorporate special environments for the crystal, such as variable temperature or high pressure. The shutter must be capable of very short, accurately timed exposures, *e.g.* 5–50 ms. As detector, films, or rather packs of four to six films with attenuators between, have been used for a large proportion of the Laue diffraction work up until now. This may seem 'old fashioned', but the combination of speed, pixel size (down to 25 μm with current scanners) and large area have made it hard to beat. Image plates are now being used; they are faster than film (by a factor of *ca* 5), but the pixel size in their scanners is larger. Charge-coupled device (CCD) detectors are being developed and may well be the most appropriate in the

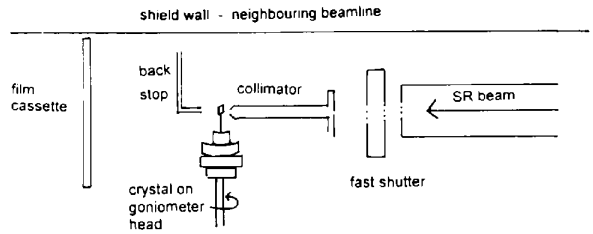

Fig. 16. Schematic drawing of experimental arrangement for recording the Laue diffraction patterns in Fig. 18. The crystal, on a goniometer head, is stationary during the short exposure, but can be turned on the spindle between exposures. To reduce the background scattering by air for very small crystals it is important that the length of the beam path in air, between collimator and backstop, is as short as possible, for example <8 mm.

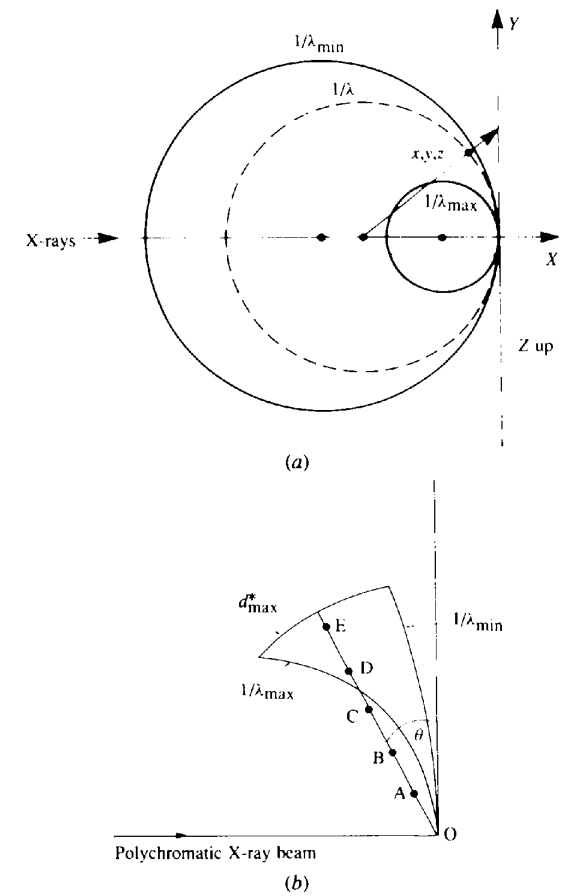

Fig. 17. (*a*) The basic geometry for Laue diffraction illustrated in relation to the reciprocal lattice (axes X, Y, Z). The point x, y, z lies on the Ewald sphere of radius $1/\lambda$ and gives rise to a spot in the Laue diffraction pattern. (*b*) The reciprocal lattice points D and E give rise to diffracted beams with the same θ, but different wavelengths; these reflections will coincide exactly on the detector, *i.e.* they give a multiple spot [from Helliwell (1992), (*a*) from p. 284, (*b*) Fig. 7.2, p. 282].

future (Allinson *et al.*, 1992). There is usually another constraint on the experimental arrangement when the full white beam is to be used without any optical elements such as mirrors in the beam line; the beam itself is very close to the shield wall of the adjacent beamline, *e.g.* 8–10 cm (on SRS station 9.7 at Daresbury), limiting the size of detectors that can be used (Fig. 16). Alternatively, the beamline optics may include focussing mirrors, in which case more space is available, but the shorter wavelengths are removed from the beam (as at SRS station 9.5 at Daresbury). Fuller accounts are given by Helliwell (1992) and elsewhere. One major driving force for the development has been the possibility of doing time-resolved experiments, which may examine individual steps of a biochemical reaction such as that between enzyme and substrate in the crystal.

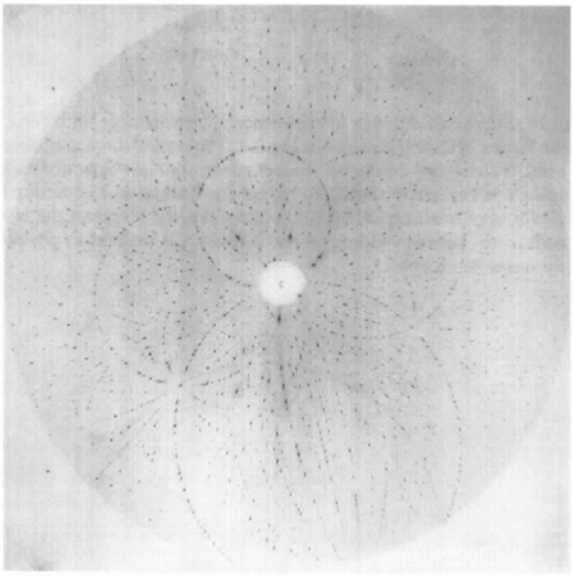

(*a*)

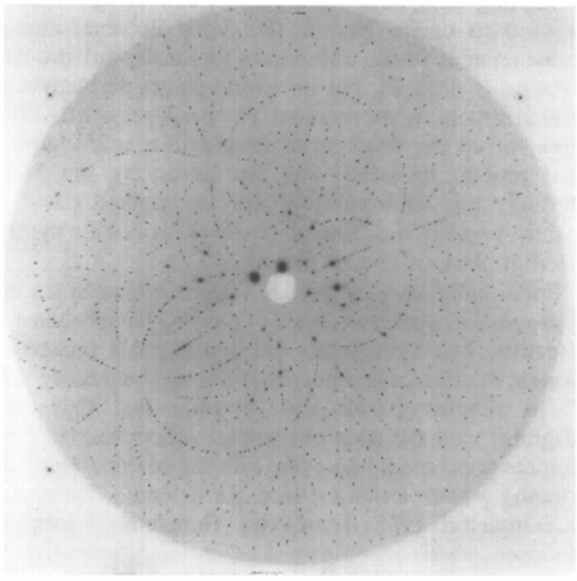

(*b*)

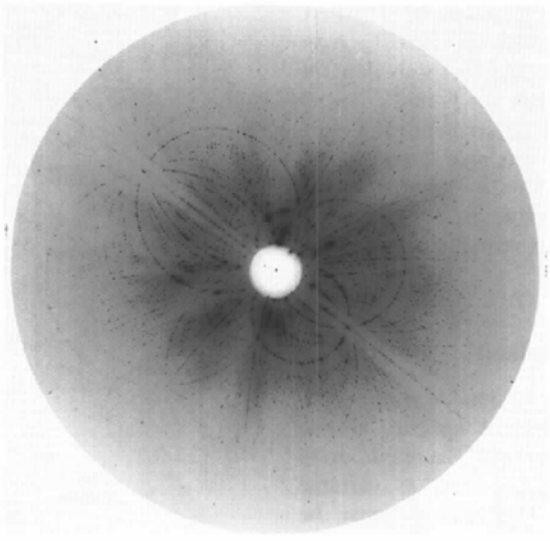

(*c*)

Fig. 18. Examples of Laue diffraction patterns recorded at Daresbury Laboratory, workstation 9.7. (*a*) For a lanthanum complex $[La_3L(OH)_2(NO_3)_4].7H_2O$, where L is a macrocyclic ligand, $C_{36}H_{42}O_3N_9$, crystal film distance 57 mm, crystal larger than collimator (0.2 mm), exposure 0.2 s with 0.2 mm Al attenuator in beam. (*b*) For an organometallic compound of composition $C_{30}H_{32}P_2O_6Ru$, crystal film distance 62 mm, crystal larger than collimator (0.2 mm), exposure 0.2 s with 0.2 mm Al attenuator in beam. (*c*) For an organometallic complex of gold and osmium (details in Table 2), crystal film distance 61 mm, crystal 0.27 × 0.06 × 0.04 mm, exposure 14 s with 0.2 mm Al + 0.114 mm Cu attenuators in beam.

The basic geometry is illustrated in Fig. 17. Any reciprocal lattice point lying between the reflecting spheres corresponding to λ_{max} and λ_{min} will give rise to a reflection, which will be recorded if θ is less than the maximum allowed by the detector. Some multiple spots arise because reflections nh, nk, nl, for several values of n, which lie on central rows of the reciprocal lattice, have identical angles of diffraction, but correspond to different wavelengths, λ/n. Cruickshank, Helliwell & Moffat (1987) have analysed the distribution of these multiple reflections and shown that up to 83% of reflections can normally be recorded as singles.

Several examples of real Laue diffraction patterns are shown in Fig. 18. The simulated pattern in Fig. 19 is colour coded to show how the spots in the Laue diffraction pattern in Fig. 18(*a*) represent different wavelengths, with a preponderance of short wavelengths near the centre of the pattern. The simulations in Fig. 20 illustrate the effects of changing crystal orientation, or of a change in the minimum observable d-spacing in the crystal. Many real patterns are recorded with the crystal in an arbitrary orientation; this turns out to be much more useful both for initial indexing of the patterns and for recording of a larger proportion of the independent reflections. The Laue photographs contain large numbers of spots. The number actually recorded depends on crystal cell and orientation, λ_{max} and λ_{min} (which are not, in the real experimental conditions, sharp cut-offs), and $d_{min} = \lambda/2\sin\theta_{max}$ for the crystal (again not a sharp cut-off). The proportion of unique reflections which can be recorded in one Laue diffraction pattern under specified conditions is shown in Table 3. Laue diffraction is a particularly attractive option for high-symmetry crystals, where one exposure can record such a high proportion of the unique data.

Fig. 19. Simulation of Laue diffraction pattern corresponding to Fig. 18(*a*). The colours of the diffraction spots represent the different wavelengths present, between 0.25 Å (blue), through the colours of the rainbow, and 1.5 Å (red). For multiple spots the longest wavelength present is shown.

Table 3. *Fraction of unique reflections recorded on one Laue film*

Calculated for a crystal film distance 60 mm, $d_{min} = 2.0$, $\lambda_{min} = 0.3$ and $\lambda_{max} = 1.7$ Å.

	One film	Two films
Crystal system	Optimum orientation	Well chosen orientations
Triclinic	0.25	0.40–0.45
Monoclinic	0.45	0.65–0.70
Orthorhombic	0.65	0.80–0.85
Tetragonal 4/*mmm*	0.88	0.90–0.95
Hexagonal 6/*mmm*	>0.90	>0.95

Laue intensity measurements and their validity

Software for processing the digitized Laue film images to yield reflection intensities has been extensively developed. The Daresbury software suite is widely used and is described by Helliwell *et al.* (1989) and Campbell (1993); other software has been used by Bartunik, Bartsch & Huang (1992) and by Smith Temple (1989). In the Daresbury software it is assumed that the unit cell is known, at least approximately. It finds and refines the crystal orientation together with other parameters such as crystal-film distance. The soft limits λ_{min}, λ_{max} and d_{min} are adjusted to give the best match with the observations. Optical densities are then integrated around each predicted spot position, with a background estimated from a ring of pixels around the spot. For film packs, wavelength-dependent interfilm scale factors are evaluated and applied, but this step is not necessary with image plates. Finally, a wavelength normalization function is established and applied, to allow for the variation of incident intensity, sample diffracting power and detector response with wavelength. Merging R-factors in the 5–10% region, together with comparisons with monochromatic diffractometer data for several protein data sets, show that the Laue method, when carefully used, can give good quality diffraction data, although not yet quite as good as the best diffractometer data. Helliwell, Gomez de Anderez, Habash, Helliwell & Vernon (1989) showed that the structure of a modest-sized organic compound, $C_{25}H_{20}N_2O_2$, in space group $P2_12_12_1$, could be solved and refined with Laue data; the H atoms could be located from a difference map and the final R factor was 0.053 for 1914 (single) reflections with $I > 2\sigma(I)$. Other structures solved entirely from Laue data (see below) give further evidence that the accuracy of the intensity measurements is satisfactory, and this is also shown by the location of a single water molecule in a difference electron-density map calculated from Laue data for human carbonic anhydrase (Lindahl, Lilias, Habash, Harrop & Helliwell, 1992).

The Laue method: some other considerations

Considerable effort has recently been given to deconvoluting the intensities measured for the multiple Laue spots, to give the individual components (Hao, Campbell, Harding & Helliwell, 1993; Campbell & Hao, 1993). These components are predominantly low-order reflections and reflections in special planes and lines in the reciprocal lattice, for example *h*00, *hk*0 or *hhh* reflections. This deconvolution procedure has a formal resemblance to that needed in powder diffraction when peaks are overlapped (Estermann & Gramlich, 1993), and it is possible that maximum entropy methods may be useful for both. Solution and refinement for a number of small molecule structures has been achieved with the single reflections only, but there are many situations where components of the multiples are important, for example in direct methods for more complicated molecules and in electron-density difference maps for proteins. It should be noted that when Laue data is

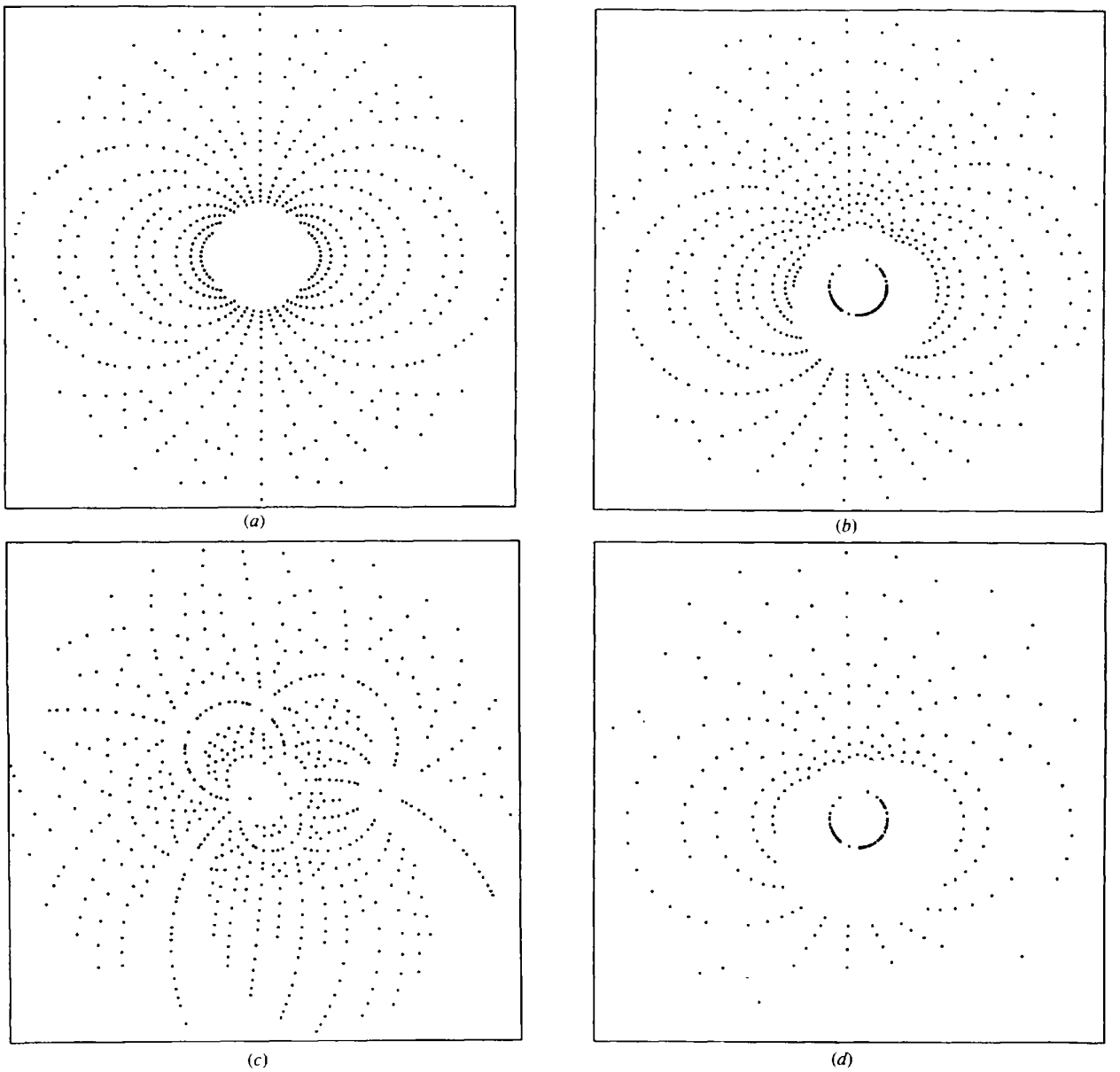

Fig. 20. Simulations of Laue diffraction patterns to illustrate the effect of crystal rotation and of change in d_{min} ($= \lambda/\sin\theta_{max}$). All simulations are for a crystal with $a = 10$ Å, parallel to the X-ray beam, $b = 8$ and $c = 14$ Å, crystal film distance 60 mm, pattern diameter 120 mm, $\lambda_{max} = 1.40$ Å. (*a*) *b* is horizontal, *c* is vertical, $\lambda_{min} = 0.2$ Å, $d_{min} = 1.0$ Å; (*b*) crystal rotated 6° about horizontal axis, and 2° around vertical axis, otherwise same as in (*a*); (*c*) crystal rotated 26° about horizontal axis and 12° around vertical axis, otherwise same as in (*a*); (*d*) d_{min} increased to 1.4 Å, otherwise same as in (*b*); note how the pattern becomes sparser, but still extends to the edge of the film.

measured from one or a small number of crystal orientations to give a large fraction of the unique reflections, the missing reflections will be mostly of low order.

Improvements continue to be made in the Laue software, notably for the handling of difficult spot shapes (Greenhough & Shrive, 1994) and towards greater automation of the software (Campbell, Clifton, Harding & Hao, 1995).

A procedure has been developed for determining unit-cell dimensions from Laue diffraction patterns (Carr, Dodd & Harding, 1993). The unit-cell angles and the relative values of a, b and c can be found by converting a Laue diffraction pattern to the form known as a gnomonic projection and identifying a prominent triangle of spots (Carr, Cruickshank & Harding, 1992); one pattern for the crystal in a general orientation should generally be sufficient to give all six quantities. To obtain a, b and c on an absolute scale an attenuator with a suitable absorption edge, for example Pd, is placed in the incident beam; λ_{min} becomes a sharp limit and can be identified and used to give the required scaling factor.

Due to the much higher intensities, radiation damage is more often a hazard in the Laue method than in monochromatic work, but, paradoxically, the Laue method may allow more intensity measurements to be made from one crystal before it has deteriorated to an unacceptable extent. Radiation damage reduces the crystal perfection, effectively increasing the mosaic spread; the Laue geometry is particularly sensitive to mosaic spread and the spots become more and more streaked, as shown in the example in Fig. 21. In general, proteins are more susceptible than organic and organometallic crystals, and these in turn are more susceptible than inorganic crystals. Removal of the longer wavelengths, say >1.2 Å, from the incident beam by a suitable attenuator enormously improves crystal lifetimes in the beam. This is essential when studying many small crystals.

Applications of the Laue method

Laue data have been recorded for a number of crystals to test the validity of the experimental method and the software. The greatest potential of the method is for time-resolved experiments, and for experiments in special environments at high temperature and/or pressure; it may also have uses for small crystals, or for crystals with a limited lifetime.

The structure of a complex molybdosulfate, $Mo_5S_2O_{23}(NEt_4)_4.PhCN$, was established with intensity data from seven Laue film packs (Maginn, Harding & Campbell, 1993). The crystal was rather small for a conventional diffractometer, but an approximate cell was derived from very weak Weissenberg photographs. The constitution was completely unknown initially (an MoS_4 complex was expected!), but direct methods and successive electron-density maps revealed it clearly. Refinement initially gave $R = 0.13$ for 2858 reflection intensities, and then after an absorption correction procedure was developed, $R = 0.10$. This R factor is admittedly high, although the structure appeared to be chemically correct. All the structure factors had been calculated using atom scattering factors without anomalous dispersion corrections. The intensity measurements were made with wavelengths in the range $\lambda = 0.49$–0.91 Å. Over this range there is a significant variation of f_{Mo} because of the anomalous dispersion contributions (see Fig. 15); at the time we had no way of including this in the structure-factor calculations, but we think that had we done so R would have improved.

For another small organometallic crystal, $AuOs_3C_{51}H_{37}P_3O_8.PF_6$ (see Fig. 22), Laue diffraction

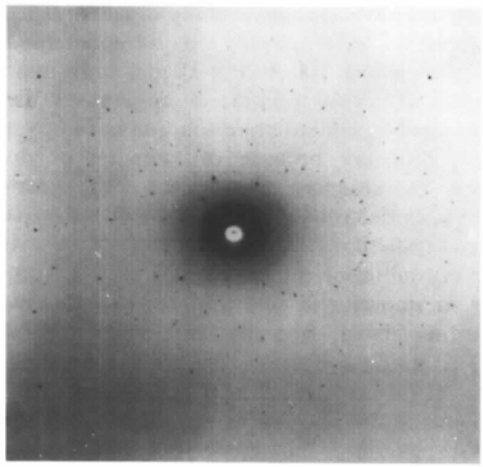

(*a*)

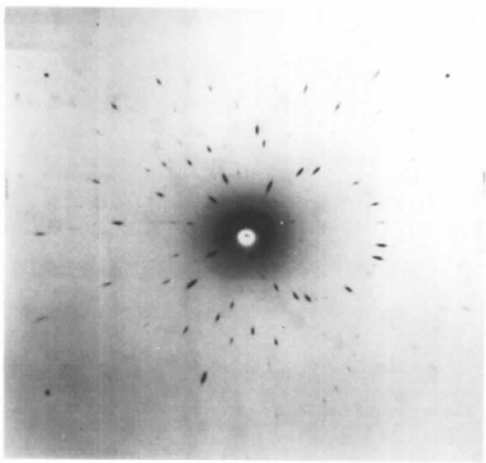

(*b*)

Fig. 21. Radiation damage in a sucrose crystal of dimensions $135 \times 90 \times 55$ μm. (*a*) 1 s exposure with a fresh crystal and (*b*) 1 s exposure of the same crystal after it had received 20 s of irradiation. SRS at 150 mA, no beam attenuation. A crystal 1/20 of this volume would require a 20 s exposure to give a pattern of similar intensity, but would be significantly damaged within this time in an unattenuated beam.

patterns provided the unit cell as well as the intensity measurements, the chemical constitution was established, and the structure refinement included allowance for anomalous dispersion. We are grateful to Professor George Sheldrick for making such refinement possible in *SHELXL*93 (Sheldrick, 1993), which gave $R = 0.078$, $wR_2 = 0.19$ for 10 625 reflection intensities measured with wavelengths in the range 0.24–0.65 Å (Dodd, Hao, Harding & Prince, 1994). Anomalous dispersion effects were also taken into account in another structure refinement with Laue intensity data, in this case for a non-centrosymmetric, but normal-sized crystal of a known compound, $RuC_{30}H_{32}P_2P_6$; this gave $R = 0.075$ for 7241 reflection intensities (wavelengths 0.42–1.04 Å) and allowed the enantiomorph to be correctly established.

Laue diffraction patterns can be recorded and measured for crystals substantially smaller than these, for example, we have intensity data for an aluminophosphate of dimensions $100 \times 20 \times 10\,\mu m$, and a mineral of dimensions $200 \times 60 \times 5\,\mu m$; in both cases the data looks reasonable, but structure solution has not yet been achieved, probably because of twinning or disorder problems. The structure of a copper hydroxycarbonate has been fully determined from Laue diffraction patterns from a crystallite of dimensions $20 \times 20 \times 10\,\mu m$; another crystallite of dimensions $20 \times 20 \times 5\,\mu m$, present as an impurity in this sample, was convincingly identified as $PbCO_3$ from its Laue diffraction patterns [Fig. 23 (Harding & Kariuki, 1995)]. Ohsumi, Hagiya & Ohmasa (1991) chose the Laue method for their experiments at the Photon Factory, Japan, to detect the diffraction patterns of minute molybdenum particles. The particles were spheres of diameter 0.8 μm, the wavelength range 0.25–2.5 Å, and the collimation system was very carefully designed to reduce the background scattered radiation. They were able to detect and measure up to 14 reflection intensities, sufficient to show that one particle was a single crystal and the other was twinned. A wavelength normalization function derived from another larger crystal was used. Diffraction peaks for even smaller volumes of crystalline bismuth filaments, $0.38\,\mu m^3$, were recorded by Skelton *et al.* (1991); they used an energy dispersive mode of recording the peaks, and were able to make deductions about lattice strain from the peak widths.

The use of Laue intensity measurements for time-resolved experiments has been attempted mainly in the protein crystallography area. The prospects appear exciting, since a substantial proportion of all the theoretically accessible reflection intensities can be recorded in one very short exposure. We have studied crystals of the cyclic phosphonitrilic chloride, $P_4N_4Cl_8$ (kindly supplied by Professor K. Venkatesan, who suggested their interest), as they are heated in a small furnace (Carr, Cheetham, Harding & Rule, 1992). The compound occurs in two crystalline forms, a metastable form in which the eight-membered P_4N_4 ring adopts a boat conformation with molecular symmetry $\bar{4}$, and a stable form in which the ring has a chair conformation with molecular symmetry $\bar{1}$. When the metastable boat form crystal is heated to *ca* 338 K, transformation to the chair form crystal occurs with very little change in cell dimensions or molecular packing; the quality of the single crystal and the diffraction pattern remains good. It was practical to record diffraction patterns at intervals of

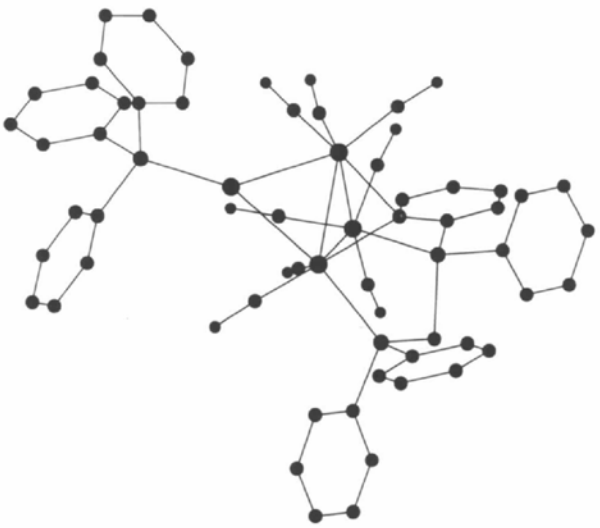

Fig. 22. The structure of the organometallic cation $AuOs_3H(CO)_8\{Ph_2PCH_2P(Ph)C_6H_4\}(PPh_3)$ established entirely from Laue diffraction photographs of a small crystal of its hexafluorophosphate. Space group *C*2/*c*. The large circles represent Au or Os atoms; the others in order of decreasing size are P, C and O.

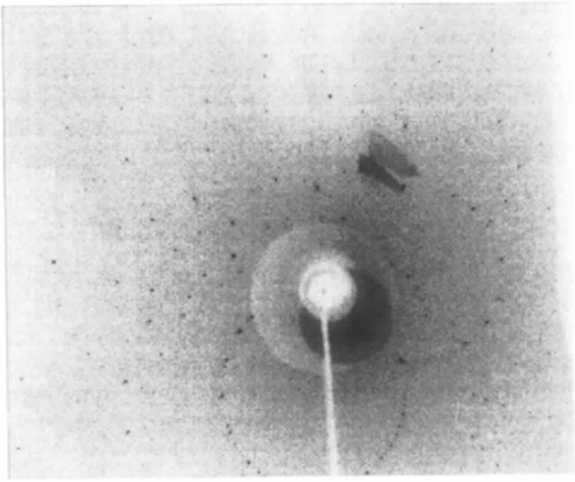

Fig. 23. Laue diffraction pattern recorded on an image plate at Daresbury for a crystal fragment of dimensions $20 \times 20 \times 5\,\mu m$, present as an impurity in a copper hydroxycarbonate sample; crystal to image plate distance 83 mm, exposure 6 s with 0.2 mm Al + 0.038 mm Cu attenuators in beam. From the positions of *ca* 100 spots in this pattern the crystallite could be identified as $PbCO_3$. Four other Laue diffraction patterns at different orientations confirmed this identification. (The dark shadows are the result of unintended scattered radiation.)

5° in temperature and 2–3 min in time, and to process these to give 200–400 unique reflection intensities from each. Full structural interpretation of the data has been more difficult; the transformation does not occur completely at the reported transition temperature, and the data suggest that a proportion of the molecules remain in the boat form up to temperatures of *ca* 373 K.

To make full use of the Laue method for time-resolved studies poses several challenges. First, if a nearly continuous series of diffraction patterns is to be recorded, the crystal quality or perfection must remain good throughout. Thus, cell dimensions and molecular packing should undergo minimal change. Second, it must be remembered that the diffraction pattern will give information on the average structure through the whole crystal and so it may be necessary to devise methods of initiating the change in all unit cells simultaneously. Third, the time scales of real transformations or reactions need to be considered. Individual chemical steps, or bond making or breaking occur in times of the order of a ps; intermediates in a reaction may have lifetimes of ms or longer.

For a small protein sample, Moffat and colleagues (Szebenyi *et al.*, 1992; see also Ren & Moffat, 1994) have achieved Laue diffraction patterns with measurable intensities recorded with one pulse of synchrotron radiation of duration 120 ps. This work, performed at Cornell, involved both detector development and development of the undulator system to give the extremely intense radiation. The undulator is a prototype for one to be installed at the Advanced Photon Source (APS) at Argonne National Laboratory, and with it even shorter exposure times may be possible. Protein crystallographers are interested in studying enzyme–substrate interactions within the crystal. These could be initiated by diffusing the substrate solution into the crystal, but in many cases this is slow compared with the time-scale of the reaction. Instead, the reaction may be initiated by a pH jump, or in other cases the substrate in a 'caged' form, *i.e.* an unreactive chemical derivative has been diffused into the crystal before the experiment and then released by a pulse of UV light. Several groups have thus succeeded in obtaining electron-density maps showing short-lived reaction intermediates bound to the enzyme (Singer, Smalas, Carty, Mangel & Sweet, 1993; John *et al.*, 1993; Duke *et al.*, 1992; Duke, Wakatsuki, Hadfield & Johnson, 1994; Cruickshank, Helliwell & Johnson, 1992). Thus, in many cases time-resolved Laue diffraction experiments will require quite extensive design and preparation, but when this is done the rewards should be great.

Thus, SR has already allowed the investigation of a variety of problems in structural chemistry which were not practical with conventional radiation sources, structures determined for small crystals and crystalline powders, or fine details revealed by data of particularly high accuracy, or structural information from samples at high temperatures and/or pressures. Some time-resolved experiments have been carried out with powders and some with protein crystals. The future should allow more of all these, and among them the time-resolved ones seem to be the most exciting. There will be other areas too, for example, the development of microdiffraction systems, or the use of the background diffuse scattering to give information on correlated atomic motions within the molecule.

I am grateful to SERC UK for financial support and synchrotron radiation facilities, to Drs B. M. Kariuki, Hao Quan, P. D. Carr, S. M. Prince, P. J. Rizkallah, S. J. Andrews, J. M. Hails, S. J. Maginn, G. M. T. Cheetham, R. J. Rule and I. M. Dodd at Liverpool University, whose work has contributed to this account, and to many other colleagues, particularly Dr J. W. Campbell at Daresbury Laboratory and Professor J. R. Helliwell at Manchester University for discussions and advice.

References

ALLINSON, N. M., COLAPIETRO, M., HELLIWELL, J. R., MOON, K. J., THOMPSON, A. W. & WEISGERBER, S. (1992). *Rev. Sci. Instrum.* **63**, 664–666.

BACHMANN, R., KOHLER, H., SCHULZ, H. & WEBER, H. P. (1985). *Acta Cryst.* A**41**, 35–40.

BARTUNIK, H. D., BARTSCH, H. H. & HUANG, Q. (1992). *Acta Cryst.* A**48**, 180–188.

BILDERBACK, D. H., THIEL, D. J., PAHL, R. & BRISTER, K. E. (1994). *J. Synchrotron Rad.* **1**, 37–42.

CAMPBELL, J. W. (1993). Daresbury Laue Software Suite, Documentation. SERC Daresbury Laboratory, Warrington WA4 4AD, England.

CAMPBELL, J. W. & HAO, Q. (1993). *Acta Cryst.* A**49**, 889–893.

CAMPBELL, J. W., CLIFTON, I. J., HARDING, M. M. & HAO, Q. (1995). *J. Appl. Cryst.* Submitted.

CARR, P. D., CHEETHAM, G. M. T., HARDING, M. M. & RULE, R. J. (1992). *Phase Transit.* **39**, 33–43.

CARR, P. D., CRUICKSHANK, D. W. J. & HARDING, M. M. (1992). *J. Appl. Cryst.* **25**, 294–308.

CARR, P. D., DODD, I. M. & HARDING, M. M. (1993). *J. Appl. Cryst.* **26**, 384–387.

CATLOW, C. R. A. & GREAVES, G. N. (1990). Editors. *Applications of Synchrotron Radiation.* Glasgow and London: Blackie.

CHEETHAM, A. K. & WILKINSON, A. P. (1992). *Angew. Chem. Int. Ed. Engl.* **31**, 1557–1570.

CHEETHAM, G. M. T., HARDING, M. M., HAGGITT, J. L., MINGOS, D. M. P. & POWELL, H. R. (1993). *J. Chem. Soc. Chem. Commun.* pp. 1000–1001.

CHRISTIDES, C., THOMAS, I. M., DENNIS, T. J. S. & PRASSIDES, K. (1993). Daresbury Laboratory Annual Report for 1992/3, Synchrotron Radiation, (p. 39). SERC Daresbury Laboratory, Warrington WA4 4AD, England.

CLARK, S. M. & DOORHYEE (1992). *J. Phys. Condens. Matter*, **4**, 8969–8974.

COPPENS, P. (1992). *Synchrotron Radiation Crystallography.* London: Academic Press.

COX, D. (1992). In *Synchrotron Radiation Crystallography.* London: Academic Press.

CROMER, D. T. & LIBERMAN, D. (1970). *J. Chem. Phys.* **53**, 1891–1898.

CRUICKSHANK, D. W. J., HELLIWELL, J. R. & JOHNSON, L. N. (1992). Editors. Time resolved macromolecular crystallography, A Royal Society Discussion Meeting, *Phil. Trans. R. Soc. London*, **340**, 169–334.

CRUICKSHANK, D. W. J., HELLIWELL, J. R. & MOFFAT, K. (1987). *Acta Cryst.* A**43**, 656–674.
DAUTER, Z., SIEKER, L. C. & WILSON, K. S. (1992). *Acta Cryst.* B**48**, 42–59.
DODD, I. M., HAO, Q., HARDING, M. M. & PRINCE, S. M. (1994). *Acta Cryst.* B**50**, 441–447.
DUKE, E. M. H., HADFIELD, A., WALTERS, S., WAKATSUKI, S., BRIAN, R. K. & JOHNSON, L. N. (1992). *Phil. Trans. R. Soc. London Ser. A*, **340**, 245–261.
DUKE, E. M. H., WAKATSUKI, S., HADFIELD, A. & JOHNSON, L. J. (1994). *Protein Sci.* **3**, 1178–1196.
ESTERMANN, M. A. & GRAMLICH, V. (1993). *J. Appl. Cryst.* **26**, 396–404.
FITCH, A. N. & JOBIC, H. (1993). *J. Chem. Soc. Chem. Commun.* pp. 1516–1517.
GREENOUGH, T. J. & SHRIVE, A. K. (1994). *J. Appl. Cryst.* **27**, 111–121.
GOMEZ DE ANDEREZ, D., HELLIWELL, M., HABASH, J., DODSON, E. J., HELLIWELL, J. R., BAILEY, R. D. & GAMMON, R. E. (1989). *Acta Cryst.* B**45**, 482–488.
HAO, Q., CAMPBELL, J. W., HARDING, M. M. & HELLIWELL, J. R. (1993). *Acta Cryst.* A**49**, 528–531.
HARDING, M. M. & KARIUKI, B. M. (1994). *Acta Cryst.* C**50**, 852–854.
HARDING, M. M. & KARIUKI, B. M. (1995). In preparation.
HARDING, M. M., KARIUKI, B. M., CERNIK, R. & CRESSEY, G. (1994). *Acta Cryst.* B**50**, 673–676.
HARDING, M. M., KARIUKI, B. M., MATHEWS, J. A., SMITH, A. K. & BRAUNSTEIN, P. (1994). *J. Chem. Soc. Dalton Trans.* pp. 33–36.
HASNAIN, S. S., HELLIWELL, J. R. & KAMITSUBO, H. (1994). Editors. *J. Synchrotron Rad.* Inaugural Issue.
HAUSERMANN, D. & BARNES, P. (1992). *Phase Transit.* **39**, 99–115.
HELLIWELL, J. R. (1992). *Macromolecular Crystallography with Synchrotron Radiation*. Cambridge Univ. Press.
HELLIWELL, J. R., HABASH, J., CRUICKSHANK, D. W. J., HARDING, M. M., GRENNHOUGH, T. J., CAMPBELL, J. W., CLIFTON, I. J., ELDER, M., MACHIN, P. A., PAPIZ, M. Z. & ZUREK, S. (1989). *J. Appl. Cryst.* **22**, 483–497.
HELLIWELL, M., GOMEZ DE ANDEREZ, D., HABASH, J., HELLIWELL, J. R. & VERNON, J. (1989). *Acta Cryst.* B**45**, 591–596.
HENDRICKSON, W. A., PAHLER, A., SMITH, J. L., SATOW, Y., MERRITT, E. A. & PHIZACKERLEY, R. P. (1989). *Proc. Natl. Acad. Sci. USA*, **86**, 2190–2194.
HESTER, J. R., MASLEN, E. N., SPADACCINI, N., ISHIZAWA, N. & SATOW, Y. (1993). *Acta Cryst.* B**49**, 842–846.
JOHN, H., RENSLAND, H., SCHLICHTING, I., VETTER, I., BORASIO, G. D., GOODY, R. S. & WITTINGHOFFER, A. (1993). *J. Biol. Chem.* **268**, 923–929.
KASSNER, D., BAUR, W. H., JOSWIG, W., EICHORN, K., WENDSCHUH-JOSTIES, M. & KUPCIK, V. (1993). *Acta Cryst.* B**49**, 646–654.
LEHMANN, C. W., BUSCHMANN, J., LUGER, P., DEMOULIN, C., FUHRHOP, J. H. & EICHORN, K. (1990). *Acta Cryst.* B**46**, 646–650.
LINDAHL, M., LILIAS, A., HABASH, J., HARROP, S. & HELLIWELL, J. R. (1992). *Acta Cryst.* B**48**, 281–285.
MAGINN, S. J., HARDING, M. M. & CAMPBELL, J. W. (1993). *Acta Cryst.* B**49**, 520–524.
MCCUSKER, L. B. (1988). *J. Appl. Cryst.* **21**, 305–310.
MCCUSKER, L. B. (1991). *Acta Cryst.* A**47**, 297–313.
MCCUSKER, L. B., BAERLOCHER, C., JAHN, E. & BULOW, M. (1991). *Zeolites*, **11**, 308–313.
MESSERSCHMIDT, A. & PFLUGRATH, J. W. (1987). *J. Appl. Cryst.* **20**, 306–315.
MIEHE, G., VOGT, T., FUESS, H. & MULLER, U. (1993). *Acta Cryst.* B**49**, 745–754.
NELMES, R. J. & MCMAHON, M. I. (1994). *J. Synchrotron Rad.* **1**, 69–73.
NIELSEN, F. S., LEE, P. & COPPENS, P. (1986). *Acta Cryst.* B**42**, 359–364.
OHSUMI, K., HAGIYA, K. & OHMASA, M. (1991). *J. Appl. Cryst.* **24**, 340–348.
PAPIZ, M. Z. (1989). Personal communication.
PAWLEY, G. S. (1981). *J. Appl. Cryst.* **14**, 357–361.
PETRICEK, V., GAO, Y., LEE, P. & COPPENS, P. (1990). *Phys. Rev. B*, **42**, 387–392.
REN, R. & MOFFAT, K. (1994). *J. Synchrotron Rad.* **1**, 78–82.
RIECK, W., EULER, H., SCHULZ, H. & SCHILDKAMP, W. (1988). *Acta Cryst.* A**44**, 1099–1101.
RIZKALLAH, P. J., HARDING, M. M., LINDLEY, P. F., AIGNER, A. & BAUER, A. (1990). *Acta Cryst.* B**46**, 262–266.
RULE, R. J. (1990). PhD thesis, Liverpool Univ., England.
SHELDRICK, G. M. (1993). *SHELXL93. Program for the Refinement of Crystal Structures*. Univ. of Göttingen, Germany.
SIMMEN, A. & MCCUSKER, L. B. (1992). Personal communication.
SINGER, P. T., SMALAS, A., CARTY, R. P., MANGEL, W. F. & SWEET, R. M. (1993). *Science*, **259**, 669–673.
SKELTON, E. F., AYERS, J. D., QUADRI, S. B., MOULTON, N. E., COOPER, K. P., FINGER, L. W., MAO, H. K. & HU, Z. (1991). *Science*, **253**, 1123–1125.
SMITH TEMPLE, B. R. (1989). PhD Thesis, Cornell Univ., Ithaca, NY, USA.
SWEET, R. M. & WOODHEAD, A. D. (1989). Editors. *Synchrotron Radiation in Structural Biology*. New York: Plenum Press.
SZEBENYI, D. M. E., BILDERBACK, D. H., LEGRAND, A., MOFFAT, K., SCHILDKAMP, W., TEMPLE, B. S. & TENG, T.-Y. (1992). *J. Appl. Cryst.* **25**, 414–423.
TEMPLETON, D. H., TEMPLETON, L. K., PHILLIPS, J. C. & HODGSON, K. O. (1980). *Acta Cryst.* A**36**, 436–442.
TEMPLETON, L. K. & TEMPLETON, D. H. (1988). *J. Appl. Cryst.* **21**, 558–561.
WALKER, R. P. (1986). Daresbury Laboratory Preprint DL/SCI/P513A. Daresbury Laboratory, Warrington WA4 4AD, England.
WILKINSON, A. P., CHEETHAM, A. K. & COX, D. E. (1991). *Acta Cryst.* B**47**, 155–161.